A Fast Algorithm for Multiphase Image Segmentation: The Split-Bregman-Projection Algorithm

Cunliang Liu, Yongguo Zheng, Zhenkuan Pan, and Guodong Wang

Abstract—**In this paper, we propose a variational model of multiphase image segmentation using n binary label functions for n regions. This framework is subject to a constraint to avoid the vacuum and overlapping problem. Firstly, we solve the simple problem without the constraint. In order to improve the computation efficiency of the unconstrained problem, we design the Split Bregman algorithm in the alternating minimization, which transforms the unconstrained model into a series of simple Euler-Lagrange equations. These equations are solved via Gauss-Seidel iterative method or expressed as generalized thresholding formulas in analytical forms. Secondly, we project the results above onto the constraint using Lagrange multiplier method. Due to the linear structure of the constraint, we can also solve the projection scheme quickly. Finally, numerical results on 2D and 3D images demonstrate that our proposed Split-Bregman-Projection (SBP) algorithm is competitive in terms of quality and efficiency compared to other methods.**

Index Terms—**Active contour model, lagrange multiplier, split bregman, binary label function, multiphase segmentation**

I. Introduction

The task of image segmentation is to partition an image into a finite number of regions according to different image properties. Multiphase image segmentation can be considered the extension from two phase segmentation. Due to the significance in various image processing applications such as in medical image analysis [1], image segmentation has received more and more attention by researchers in recent years. One of the important problems of image segmentation is how to design the characteristic function of each region.

In general, the existing characteristic functions can be categorized into three classes. The first class is designed using the concept of Gamma-convergence [2]-[4] and the classic Mumford-Shah model [5]. The second one expresses the active contours using zero level sets of signed distance functions [6]. The third one uses label functions to achieve the goal [7]. We focus on the last two classes here.

Based on reduced Mumford-Shah model and level set method, Chan and Vese [8] proposed the popular variational level set model of two phase image segmentation, usually called Chan-Vese model. It has been extended to multiphase image segmentation, such as Vese and Chan [9] used n level set functions to represent 2^n regions, Pan et al. [10] introduced n-1 level set functions for n regions, Samson et al. [11] used n level set functions for n regions, and Chung and Vese [12] used only one level set function to represent contours.

Label function methods have good correspondence with level set methods because the Heaviside expression of a level set function is a typical label function. Besides, Bresson et al. [13] proposed a binary label function for two phase image segmentation, Lie et al. proposed a scheme using n label functions for 2^n regions [14] and a scalar label function for n regions [15].

For the two phase image segmentation using a binary label function, Bresson et al. [13] verified that the global optimization can be realized based on convex relaxation and thresholding techniques, which have been used to solve the models of multiphase image segmentation [7], [16] and [18], although it has not yet the feature of globalization.

In order to improve the computation efficiency, Bresson et al. [13] designed a dual method and Goldstein et al. [17] introduced the Split Bregman algorithm for two phase image segmentation. Also, these two methods have been used to solve multiphase image segmentation [16] and [18] respectively. In this paper, we'll propose a fast algorithm for multiphase image segmentation combing the Split Bregman algorithm and constraint projection method.

The remainder of this paper is organized as follows. In Section II, some related models and algorithms are reviewed. In Section III, a variational model for multiphase image segmentation using n binary label functions for n regions is proposed and its Split-Bregman-Projection (SBP) algorithm is designed. Some experiments are given in Section IV. The concluding remarks are presented in Section V.

II. Fast Global Minimization of Two Phase Segmentation Model

A. Globally Convex Segmentation Models

Let $\Omega \subset \Re^N$ be image domain, $u_0 : \Omega \to \Re$ be a given image. The variable X in $u_0(X)$ is a point in Ω. using the Heaviside function H; the Chan-Vese model [8] of two phase image segmentation can be stated as the following variational level set formulation:

$$\min_{\phi,c_1,c_2} \left\{ \begin{array}{l} E_{CV}(\phi,c_1,c_2) = \gamma \int_\Omega |\nabla H(\phi)| dX \\ \qquad + \int_\Omega \alpha_1 (c_1 - u_0)^2 H(\phi) dX \\ \qquad + \int_\Omega \alpha_2 (c_2 - u_0)^2 (1 - H(\phi)) dX \end{array} \right\}, \quad (1)$$

where ϕ is a standard level set function. The minimization of

Manuscript received June 10, 2011; revised August 1, 2011. This work was supported in part by the Natural Science Foundation of Shandong Province (ZR2010FQ030), and in part by Shandong Province Postdoctoral Special Fund Innovative Projects (201003046).

The authors are with the College of Information Science and Engineering, Shandong University of Science and Technology, Qingdao, Shandong China, and also with the College of Information Engineering, Qingdao, Shandong China (e-mail: clliuqdu@ gmail.com; e-mail: zhengyg206@163.com; e-mail: zkpan@qdu.edu.cn; e-mail: doctorwgd@gmail.com).

(1) can be solved by the standard PDE method. Its gradient descent equation is

$$\frac{\partial \phi}{\partial t} = \delta(\phi)\left(\gamma \nabla \cdot \left(\frac{\nabla \phi}{|\nabla \phi|}\right) - \left(\alpha_1 (c_1 - u_0)^2 - \alpha_2 (c_2 - u_0)^2\right)\right), \quad (2)$$

where δ is the Delta function with $\delta(\phi) = \partial H(\phi)/\partial \phi$.

Due to the local nature of (1), its result depends on initialization of the level set function. In order to solve this problem, Bresson et al. [13] transformed (1) into a globally convex segmentation (GCS) model. We remind the general ideas.

Considering $\delta(\phi) \geq 0$, we replace $\delta(\phi)$ with 1, which does not affect the result of the evolution equation (2). This leads to the equivalent equation as follows

$$\frac{\partial \phi}{\partial t} = \gamma \nabla \cdot \left(\frac{\nabla \phi}{|\nabla \phi|}\right) - \left(\alpha_1 (c_1 - u_0)^2 - \alpha_2 (c_2 - u_0)^2\right). \quad (3)$$

The flow (3) represents the gradient descent for minimizing the energy

$$\min_{\substack{\psi, c_1, c_2 \\ \psi \in \{0,1\}}} \left\{ \begin{aligned} E^1_{GCS}(\psi, c_1, c_2) &= \gamma \int_\Omega |\nabla \psi| dX \\ &+ \int_\Omega \alpha_1 (c_1 - u_0)^2 \psi dX \\ &+ \int_\Omega \alpha_2 (c_2 - u_0)^2 (1 - \psi) dX \end{aligned} \right\}, \quad (4)$$

where ψ is a binary label function: $\psi \in \{0,1\}$. We change the notation ϕ into ψ to avoid any confusion with the standard level set function here. Equation (4) is a non-convex model due to the definition domain of ψ. The authors [13] modified it to the following convex minimization problem by relaxing the binary constraint of the label function ψ over the interval [0,1]:

$$\min_{\substack{\psi, c_1, c_2 \\ \psi \in [0,1]}} \left\{ \begin{aligned} E^2_{GCS}(\psi, c_1, c_2) &= \gamma \int_\Omega |\nabla \psi| dX \\ &+ \int_\Omega \alpha_1 (c_1 - u_0)^2 \psi dX \\ &+ \int_\Omega \alpha_2 (c_2 - u_0)^2 (1 - \psi) dX \end{aligned} \right\}. \quad (5)$$

In addition, the authors [13] used the geodesic length [19] and proposed the enhanced convex energy minimization model combining edge and region terms

$$\min_{\substack{\psi, c_1, c_2 \\ \psi \in [0,1]}} \left\{ \begin{aligned} E^g_{GCS}(\psi, c_1, c_2) &= \gamma \int_\Omega g(u_0) |\nabla \psi| dX \\ &+ \int_\Omega \alpha_1 (c_1 - u_0)^2 \psi dX \\ &+ \int_\Omega \alpha_2 (c_2 - u_0)^2 (1 - \psi) dX \end{aligned} \right\}, \quad (6)$$

where $g(u_0)$ is an edge detection function, and one common choice for the edge detector is

$$g(u_0) = \frac{1}{1 + |\nabla G_\sigma * u_0|^2}. \quad (7)$$

G_σ is a Gaussian kernel, and $G_\sigma * u_0$ is a smoother to u_0.

B. The Split Bregman Algorithm

The Split Bregman algorithm was initially introduced for solving general L1-norm problems [20]. In [17], this method was applied to the GCS model.

Energy (6) is a minimization problem with multiple variables, which is usually solved via alternating optimization technique. In each loop, we firstly fix label function ψ to minimize the functional with respect to parameter c_1 and c_2, then we fix c_1 and c_2 to solve the minimization with respect to ψ. The parameters c_1 and c_2 are estimated as

$$c_1 = \frac{\int_\Omega u_0 \psi dX}{\int_\Omega \psi dX}, \; c_2 = \frac{\int_\Omega u_0 (1 - \psi) dX}{\int_\Omega (1 - \psi) dX}. \quad (8)$$

The energy minimization with respect to ψ is

$$\min_{\psi, \psi \in [0,1]} \left\{ \begin{aligned} E^g_{GCS}(\psi) &= \gamma \int_\Omega g(u_0) |\nabla \psi| dX \\ &+ \int_\Omega \alpha_1 (c_1 - u_0)^2 \psi dX \\ &+ \int_\Omega \alpha_2 (c_2 - u_0)^2 (1 - \psi) dX \end{aligned} \right\}. \quad (9)$$

Based on [20], Goldstein et al. [17] introduced auxiliary variable $\vec{d}$ and Bregman iterative parameter $\vec{b}$ to transform (9) into the following form

$$\left(\psi^{k+1}, \vec{d}^{k+1}\right) = \arg \min_{\substack{\psi, \vec{d} \\ \psi \in [0,1]}} \left\{ \begin{aligned} &\gamma \int_\Omega g(u_0) \left|\vec{d}\right| dX \\ &+ \frac{\theta}{2} \int_\Omega \left(\vec{d} - \nabla \psi - \vec{b}^{k+1}\right)^2 dX \\ &+ \int_\Omega \left(\alpha_1 (c_1 - u_0)^2 - \alpha_2 (c_2 - u_0)^2\right) \psi dX \end{aligned} \right\}, \quad (10)$$

where $\vec{b}^{k+1} = \vec{b}^k + \nabla \psi^k - \vec{d}^k$. Using the variational method, we can obtain the Euler-Lagrange equations of ψ and $\vec{d}$ as

$$\begin{cases} \theta \nabla \cdot \left(\vec{d} - \nabla \psi - \vec{b}^{k+1}\right) + \left(\alpha_1 (c_1 - u_0)^2 - \alpha_2 (c_2 - u_0)^2\right) = 0 & in\ \Omega \\ \left(\vec{d} - \nabla \psi - \vec{b}^{k+1}\right) \cdot \vec{n} = 0 & on\ \partial\Omega \end{cases}, \quad (11)$$

and

$$\theta\left(\vec{d} - \nabla \psi^{k+1} - \vec{b}^{k+1}\right) + \gamma g(u_0) \frac{\vec{d}}{\left|\vec{d}\right|} = 0. \quad (12)$$

Equation (11) can be solved using Gauss-Seidel iterative method, and (12) can be presented as the following generalized soft thresholding formula in analytical form

$$\vec{d}^{k+1} = Max\left(\left|\nabla \psi^{k+1} + \vec{b}^{k+1}\right| - \frac{\gamma g(u_0)}{\theta}, 0\right) \frac{\nabla \psi^{k+1} + \vec{b}^{k+1}}{\left|\nabla \psi^{k+1} + \vec{b}^{k+1}\right|}, \; 0 \cdot \frac{0}{0} = 0. \quad (13)$$

Finally, the result of global minimization can be obtained via the following formula

$$\psi^* = \begin{cases} 1 & \psi \geq \eta \\ 0 & otherwise \end{cases}, for\ \forall \eta \in (0,1). \quad (14)$$

III. The Split-Bregman-Projection Algorithm

A. The Proposed Energy

Under the variational level set framework, Samson et al. [11] proposed the following level set energy minimization functional

$$\min_{c,\phi}\left\{\begin{array}{l} E_{n2n}(c,\phi)=\sum_{i=1}^{n}\gamma_i\int_{\Omega}g(u_0)\left|\nabla H(\phi_i)\right|dX \\ \quad+\sum_{i=1}^{n}\int_{\Omega}(c_i-u_0)^2H(\phi_i)dX \\ \quad+\frac{\mu}{2}\int_{\Omega}\left(\sum_{i=1}^{n}H(\phi_i)-1\right)^2dX \end{array}\right\}, \tag{15}$$

where the first term of the right-hand side of (15) is used to enforce the regularity of the interface, the second one is a data fidelity term, and the third one is a penalty term used to avoid the vacuum and overlapping problem. See [11] for more details.

Based on [20], [13] and [17], we replace the level set function ϕ_i, $i=1,...n$, by the binary label functions ψ_i, $i=1,...,n$. Hence we can rewrite (15) as the following energy

$$\min_{c,\psi}\left\{\begin{array}{l} E^{c}_{n2n}(c,\psi)=\sum_{i=1}^{n}\gamma_i\int_{\Omega}g(u_0)\left|\nabla\psi_i\right|dX \\ \quad+\sum_{i=1}^{n}\alpha_i\int_{\Omega}(c_i-u_0)^2\psi_i dX \end{array}\right\}, \tag{16}$$

where ψ_i satisfies two constraints

$$K(\psi_i)=\psi_i(\psi_i-1)=0\ (\psi_i\in\{0,1\}, i=1,...,n) \tag{17}$$

and

$$L(\psi)=\sum_{i=1}^{n}\psi_i-1=0\,. \tag{18}$$

Together with the constraints (17) and (18), energy (16) can be rewritten as the following compact form

$$\min_{\substack{c,\psi\\ K(\psi_i)=0\\ L(\psi)=0}}\left\{\begin{array}{l} E^{c}_{n2n}(c,\psi)=\sum_{i=1}^{n}\gamma_i\int_{\Omega}g(u_0)\left|\nabla\psi_i\right|dX \\ \quad+\sum_{i=1}^{n}\int_{\Omega}(c_i-u_0)^2\psi_i dX \end{array}\right\}. \tag{19}$$

B. Computation Strategy

Obviously, energy (19) is a minimization problem with constraints, which usually can be solved through Lagrange Multiplier method [14], penalty function method or augmented Lagrange method [15]. In this paper, we propose a simple and fast algorithm without introducing too many parameters as the methods mentioned above.

Firstly, we'll solve the following simple problem without the constraint (18)

$$\min_{\substack{c,\tilde{\psi}\\ K(\tilde{\psi}_i)=0}}\left\{\begin{array}{l} E^{c1}_{n2n}(c,\tilde{\psi})=\sum_{i=1}^{n}\gamma_i\int_{\Omega}g(u_0)\left|\nabla\tilde{\psi}_i\right|dX \\ \quad+\sum_{i=1}^{n}\int_{\Omega}(c_i-u_0)^2\tilde{\psi}_i dX \end{array}\right\}. \tag{20}$$

Then we use Lagrange multiplier method project $\tilde{\psi}$ onto the constraint (18), i. e.

$$\min_{\lambda,\psi}\left\{E^{c2}_{n2n}(\lambda,\psi)=\frac{1}{2}\sum_{i=1}^{n}\int_{\Omega}\left(\psi_i-\tilde{\psi}_i^{k+1}\right)^2dX+\lambda\int_{\Omega}L(\psi)dX\right\}, \tag{21}$$

where λ is the Lagrange multiplier.

C. Solving $\tilde{\psi}$ Using the Split Bregman Algorithm

After $c_i\,(i=1,2,...n)$ is estimated, we relax constraint (17) by letting $\tilde{\psi}_i\in[0,1]$ and apply the Split Bregman method to E^{c1}_{n2n}:

$$\left(\tilde{\psi}_i^{k+1},\vec{d}_i^{k+1}\right)=\arg\min_{\substack{\tilde{\psi},\vec{d}\\ \tilde{\psi}_i\in[0,1]}}\left\{\begin{array}{l} \sum_{i=1}^{n}\gamma_i\int_{\Omega}g(u_0)\left|\vec{d}_i\right|dX \\ +\frac{\theta}{2}\sum_{i=1}^{n}\int_{\Omega}(\vec{d}_i-\nabla\tilde{\psi}_i-\vec{b}_i^{k+1})^2dX \\ +\sum_{i=1}^{n}\int_{\Omega}(c_i-u_0)^2\tilde{\psi}_i dX \end{array}\right\}, \tag{22}$$

where $\vec{b}_i^{k+1}=\vec{b}_i^{k}+\nabla\tilde{\psi}_i^{k}-\vec{d}_i^{k}$. Following [17], we use the alternative minimization method to find the numerical solution for (22).

Firstly, we fix $\vec{d}_i^{k}$ to solve $\tilde{\psi}_i^{k+1}$:

$$\min_{\tilde{\psi}}\left\{\begin{array}{l} \frac{\theta}{2}\sum_{i=1}^{n}\int_{\Omega}(\vec{d}_i^{k}-\nabla\tilde{\psi}_i-\vec{b}_i^{k+1})^2dX \\ +\sum_{i=1}^{n}\int_{\Omega}\left(c_i^{k}-u_0\right)^2\tilde{\psi}_i dX \end{array}\right\}. \tag{23}$$

The solution of (23) is given by the following PDEs:

$$\left\{\begin{array}{ll} \theta\nabla\cdot\left(\vec{d}_i^{k}-\nabla\tilde{\psi}_i-\vec{b}_i^{k+1}\right)+\alpha_i\left(c_i^{k}-u_0\right)^2=0 & in\ \Omega \\ \left(\vec{d}_i^{k}-\nabla\tilde{\psi}_i-\vec{b}_i^{k+1}\right)\cdot\vec{n}=0 & on\ \partial\Omega \end{array}\right.. \tag{24}$$

We also obtain $\tilde{\psi}_i^{k+1}$ using a Gauss-Seidel method. To ensure $\tilde{\psi}_i^{k+1}\in[0,1]$, we can use the following formula:

$$\tilde{\psi}_i^{k+1}=\max\left(\min\left(\tilde{\psi}_i^{k+1},1\right),0\right). \tag{25}$$

Secondly, we fix $\tilde{\psi}_i^{k+1}$ to solve $\vec{d}_i^{k+1}$:

$$\min_{\vec{d}}\left\{\sum_{i=1}^{n}\gamma_i\int_{\Omega}g(u_0)\left|\vec{d}_i\right|dX+\frac{\theta}{2}\sum_{i=1}^{n}\int_{\Omega}(\vec{d}_i-\nabla\tilde{\psi}_i-\vec{b}_i^{k+1})^2dX\right\}. \tag{26}$$

Minimization with respect to $\vec{d}_i^{k+1}$ can be performed explicitly using the generalized soft thresholding formula:

$$\vec{d}_i^{k+1}=\max\left\{\left|\nabla\tilde{\psi}_i^{k+1}+\vec{b}_i^{k+1}\right|-\frac{\gamma_i}{\theta},0\right\}\frac{\nabla\tilde{\psi}_i^{k+1}+\vec{b}_i^{k+1}}{\left|\nabla\tilde{\psi}_i^{k+1}+\vec{b}_i^{k+1}\right|},\ 0\cdot\frac{0}{0}=0\,. \tag{27}$$

D. Projection

The Euler-Lagrange equation of the energy functional (21) is as follows:

$$\psi_i-\tilde{\psi}_i^{k+1}+\lambda=0\,. \tag{28}$$

From (18) and (28), we get

$$\psi_i^{k+1} = \tilde{\psi}_i^{k+1} - \frac{\sum_{j=1}^{n} \tilde{\psi}_j^{k+1} - 1}{n}. \quad (29)$$

At last, the final segmented regions are found by thresholding the function ψ_i to get:

$$\psi_i^* = \begin{cases} 1 & \psi_i \geq \eta \\ 0 & otherwise \end{cases}, \text{ for } \forall \eta \in (0,1). \quad (30)$$

E. Algorithm Details

The Split-Bregman-Projection minimization scheme is placed into algorithm 1, we get the following scheme for segmentation.

Algorithm 1: the Split-Bregman-Projection Scheme

– Initialization: $\vec{d}_i^0 = \vec{b}_i^0 = 0$, for $i = 1, \ldots, n$;
– while $\left| \left(E^{k+1} - E^k \right) \Big/ E^k \right| > \varepsilon$ do
– Compute $\vec{b}_i^{k+1} = \vec{b}_i^k + \nabla \tilde{\psi}_i^k - \vec{d}_i^k$;
– Compute $\tilde{\psi}_i^{k+1}$ from (24);
– Compute $\vec{d}_i^{k+1}$ from (27);
– Compute ψ_i^{k+1} from (29);
– Find ψ_i^* from (30);
– Update c_i ;
– end while

IV. Experimental Results

In this section, a large set of comparison experiments is presented to test the performance of multiphase segmentation using the proposed SBP algorithm. Our results are compared with other related works [11] and [15] in quality and efficiency. All the tests are performed on a laptop which is equipped with the Intel (R) core (TM) 2 Duo CPU E7400 @ 2.80 GHz processors and 2 GB of RAM. We build the whole system under Windows XP using MATLAB v7.0 library.

A. Parameter Settings

There are a number of parameters that must be appropriately determined. Some of them have default values. We give the description as follows: The time step and the space step used by (15) are always held as 0.2 and 1 respectively; the parameters ε and η used by (19) are fixed as 0.001 and 0.5 respectively; the other parameters should be determined manually.

For quantitative comparison of the following experimental results, the accuracy of clustering is analyzed by the Classification accuracy. All computation time are reported in seconds.

B. Comparison and Analysis of 2D Experiments

In this part, we consider two-dimensional cases and restrict ourselves to gray-scale images.

The first experiment tries to verify the superior performance of our proposed SBP algorithm over the traditional Samson et al.'s algorithm [11]. Fig. 1(e)-(j) show that our proposed SBP model improves the accuracy of clustering. Additionally, table I demonstrates that the SBP algorithm can really speed up the convergence rate of Samson et al.'s algorithm.

In Fig. 2, we compare the piecewise constant level set method (PCLSM) in [15] with our SBP algorithm. The phases of both methods are displayed in the last two rows. Our method gives better segmentation results than PCLSM does from Fig. 2(d)-(k).

In Fig. 3, we test our method with four-phase image segmentation. The image in Fig. 3(a) is available to the public at http://www.bic.mni.mcgill.ca/brainweb/. There are four classes that should be identified: cerebrospinal fluid (CSF), gray matter (GM), white matter (WM) and the background. But we do not depict the background phase here. Compared with the exact results (Fig. 3 (c)–(e)) from the website above, our results (Fig. 3 (f)–(h)) are satisfactory.

C. Comparison and Analysis of 3D Experiments

In this part, we extend our mode to three-dimensional segmentation and reconstruction.

Fig. 4 shows the 3D segmentation and reconstruction of an artificial Palace with three phases. We designed 95 2D synthetic images as the original input data for the 3D segmentation and reconstruction. We do not depict the background here. The size of each image is 150*150 pixels.

The data presented on Fig. 5 is provided by The National Library of Medicine's Visible Human Project. We select 105 2D images as the original input data. The size of each image is 150*128 pixels. There are three phases that should be identified: mandible, teeth and the background. Also, we do not depict the background phase here.

Computation time and number of iterations required for convergence are shown in table II. As can be seen, our proposed SBP algorithm is easy to extend to three-dimensional problems, and the results seem as good as for two-dimensional problems.

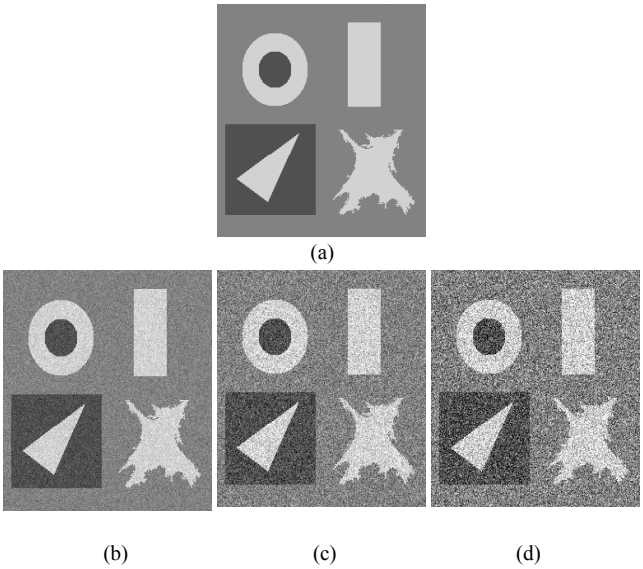

(a)

(b) (c) (d)

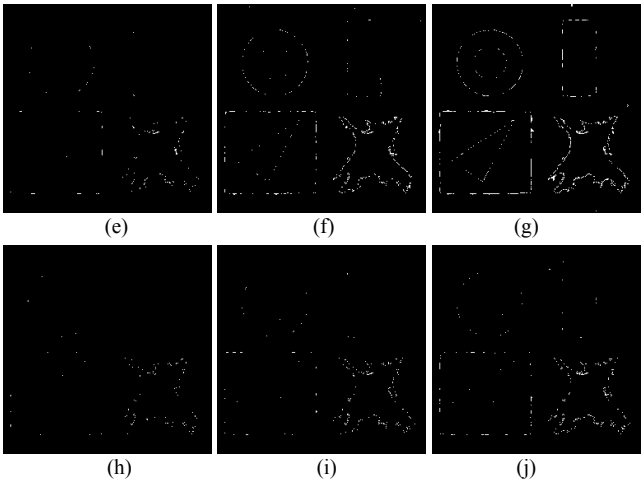

Fig. 1. Comparison of the samson et al.'s method with the SBP method on different noise levels. (a) the clean piecewise constant image; (b)–(d) images contaminated by zero mean Gaussian noise with standard device 15, 30, and 45 respectively; (e)–(g) the misclassified pixels of the Samson et al.'s method corresponding to (b)–(d) with γ = 115, 155, 200 and μ = 1500, 1600, 1800 respectively; (h)–(j) the misclassified pixels of the SBP model corresponding to (b)–(d) with γ = 25, 40, 120 and θ = 3000, 5000, 8000 respectively. The image size is 254*254 pixels.

TABLE I: ITERATIONS, COMPUTATION TIME AND ACCURACY

Solving methods	Noise figures	Iterations	Computation time	Classification accuracy
The method [11]	Fig. 1(b)	143	16.74	99.82%
	Fig. 1(c)	219	25.63	99.27%
	Fig. 1(d)	405	35.67	98.76%
The SBP method	Fig. 1(b)	13	1.30	99.84%
	Fig. 1(c)	30	2.96	99.68%
	Fig. 1(d)	35	3.49	99.51%

TABLE II: RESULTS FOR 3D SEGMENTATION AND RECONSTRUCTION

Solving methods	Figures	Iterations	Computation time
The method [11]	Fig. 4(d)	105	358.37
	Fig. 5(d)	278	947.61
The SBP method	Fig. 4(d)	9	50.26
	Fig. 5(d)	10	57.36

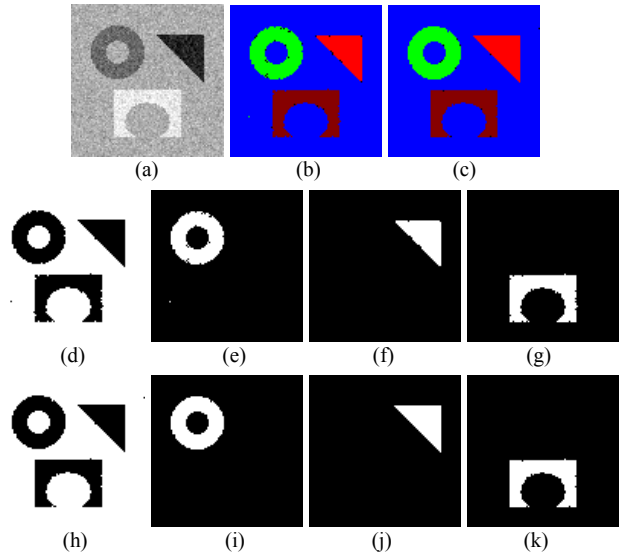

Fig. 2. Comparison of the PCLSM method and the SPB methods. (a) the noisy image; (b) the segmentation by the PCLSM method; (c) by the SBP method; (d)–(g) the four phases by the PCLSM method; (h)–(k) the label functions by the SBP method. The image size is 100*100 pixels.

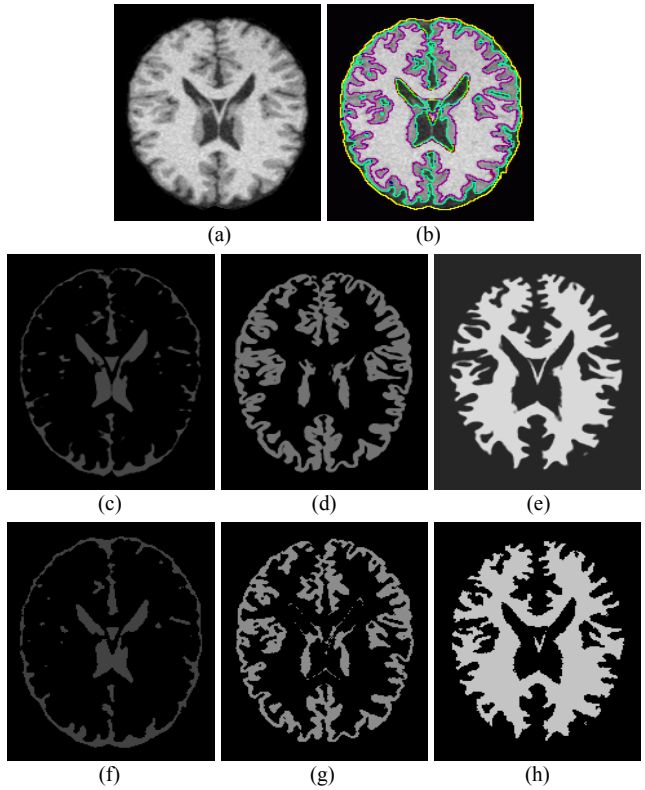

Fig. 3. Four-phase segmentation. (a) a brain MR image with noise 7% and RF-plus 20%; (b) the classification results by our proposed method; (c)-(e) the exact different tissues; (f)-(h) three phases by the SBP method. The image size is 160*200 pixels.

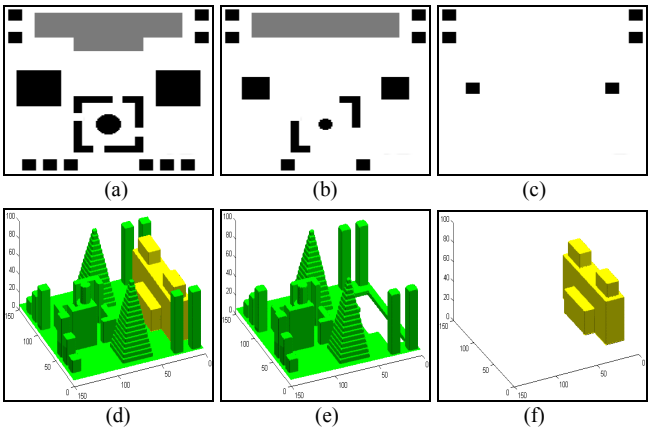

Fig. 4. 3D segmentation and reconstruction of an artificial palace. (a)-(c) the 15th, 45th and 75th image; (d) the results of 3D segmentation and reconstruction by the SBP method; (e) and (f) the different phases.

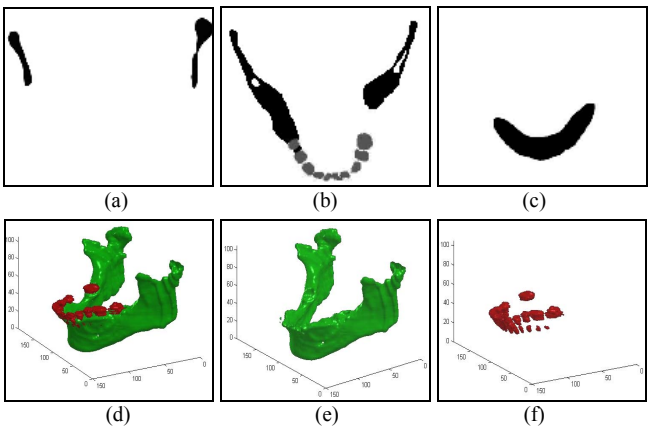

Fig. 5. 3D segmentation and reconstruction of mandible and teeth. (a)-(c) the 25th, 60th and 95th image. (d) the results of 3D segmentation and reconstruction by the SBP method. (e) and (f) the different phases.

V. Conclusion

We have presented a variational model based on the binary label functions for multiphase image segmentation. Also, we proposed an efficient and fast numerical scheme to minimize the variational segmentation framework. The proposed Split-Bregman-Projection algorithm is easy to implement and allows us to avoid the usual drawback in the some traditional approaches to ensure a correct computation. But he energy functional for our approach is locally convex, which means that proper initial guesses are needed. Future works are how to choice good initial contours and to investigate the global minimization approach of multiphase image segmentation.

References

[1] A. Yezzi, S. Kichenassamy, A. Kumar, P. Olver, and A. Tannenbaum, "A geometric snake model for segmentation of medical imagery," *IEEE Trans. on Med. Imaging*, vol. 16, pp.199-209, April 1997.

[2] L. Ambrosio and V. M. Tortorelli, "Approximation of functionals depending on jumps by elliptic functionals via Gamma-convergence," *Comm. on Pure and Appl. Math.*, vol. 43, pp. 999-1036, 1990.

[3] S. Esedoglu and Y.-H. Tsai, "Threshold dynamics for the piecewise constant Mumford-Shah functional," *Journal of Computational Physics*, vol. 211, pp. 367-384, October 2004.

[4] Y. M. Jung, S. H. Kang, and J. Shen, "Multiphase image segmentation via Modica-Mortola phase transition," *Society for Industrial and Applied Mathematics*, vol. 67, pp. 1213-1232, 2007.

[5] D. Mumford and J. Shah, "Optimal approximations by piecewise smooth functions and associated variational problems," *Comm. On Pure and Appl. Math.*, vol. 42, pp. 577-685, 1989.

[6] S. Osher and J. A. Sethian, "Fronts propagating with curvature dependent speed: Algorithms based on Hamilton-Jacobi formulations," *Journal of Computational Physics*, vol. 79, pp. 12-49, 1988.

[7] F. Li, C.-M. Shen, and C.-M. Li, "Multiphase soft segmentation with total variation and H1 regularization," *Journal of Mathematical Imaging and Vision*, vol. 37, pp. 98-111, February 2010.

[8] T. F. Chan and L. A. Vese, "Active contours without edges," *IEEE Transactions on Image Processing*, vol. 10, pp. 266–277, February 2001.

[9] L. A. Vese and T. F. Chan, "A multiphase level set framework for image segmentation using the Mumford and Shah model," *International Journal of Computer Vision*, vol. 50, pp. 271-293, 2002.

[10] Z.-K. Pan, H. Li, W.-B. Wei, Z.-B. Guo, and C.-F. Zhang, "A variational level set method of multiphase segmentation for 3D images," *Chinese Journal of Computers*, vol. 32, pp. 2464-2474, 2009.

[11] C. Samson, L. Blanc-Feraud, and G.Aubert, "A level set model for image classification," *International Journal of Computer Vision*, vol. 40, pp. 187-197, 2000.

[12] G. Chung and L. A. Vese, "Energy minimization based segmentation and denoising using a multilayer level set approach," *Lecture Notes in Computer Science*, vol. 3757, pp. 439-455, 2005.

[13] X. Bresson, S.Esedoglu, P.Vandergheynst, J. P.Thiran, and S.Osher, "Fast global minimization of the active contour/snake model," *J. Math. Imaging and Vision*, vol. 28, pp. 151-167, 2007.

[14] J. Lie, M. Lysaker, and X.-C. Tai, "A binary level set model and some applications to Mumford-Shah image segmentation," *IEEE Transection on Image Processing*, vol. 15, pp. 1171-1181, May 2006.

[15] J. Lie, M. Lysaker, and X.-C. Tai, "A variant of the level set method and applications to image segmentation," *Mathematics of Computation*, vol. 75, pp. 1155–1174, July 2006.

[16] F. Li and M. K. Ng, "Kernel density estimation based multiphase fuzzy region competition method for texture image segmentation," *Communications in Computational Physics*, vol. 8, pp. 623-641, June 2009.

[17] T. Goldstein, X. Bresson, and S. Osher, "Geometric applications of the Split Bregman Method: Segmentation and surface reconstruction," *Journal of Scientific Computing*, vol. 45, pp. 272-293, October 2010.

[18] L.-Y. Wang et al, "Alternating convex relaxation minimization of the multiphase image segmentation model and its Split Bregman algorithm," *Journal of Shandong University (Engineering Science)*, vol. 41, pp. 40-45, April 2011.

[19] V. Caselles, R. Kimmel, and G. Sapiro, "Geodesic active contours," *International Journal of Computer Vision*, vol. 22, pp. 61–79, February 1997.

[20] T. Goldstein and S. Osher, "The Split Bregman method for L1 regularized problems," *SIAM Journal on Imaging Sciences*, vol. 2, pp. 323-343, April 2008.

Cunliang Liu was born in 1977. He received the B.S. degree and M.S. degree in computer application technology from the Shenyang Ligong University, Shenyang, China, in 2000 and 2003, respectively. He is currently a lecturer in the College of Information Engineering at Qingdao University. His research interests include image segmentation, the variational methods and PDEs in image processing.

Yongguo Zheng was born in 1963. He is currently a Professor of computer science at Shandong University of Science & Technology. Zheng's research interests lie in the area of computer vision, image segmentation, object recognition, and tracking

Zhenkuan Pan was born in 1966. He received his Ph.D. degree in engineering mechanics from Shanghai Jiao Tong University, China in 1992. Currently he is a professor of the College of Information Engineering at Qingdao University. His research interests include dynamics and control of multibody systems, computer simulation and variational image processing. He has published numerous papers and conference papers in the area of image processing and object recognition.

Guodong Wang was born in 1980. He received his Ph.D degree in the Institute for Pattern Recognition and Artificial Intelligence, Huazhong University of Science and Technology, China in 2008. Currently he is a lecturer of the College of Information Engineering at Qingdao University. His research interests include image analysis and variational image processing.